Ignition and Burn in a Hybrid Nuclear Fuel for a Pulsed Rocket Engine

B. Taylor[a,b], J. Cassibry, Ph.D.[b], R. Adams, Ph.D.[a]

[a] *Advanced Propulsion Systems Department NASA Marshall Space Flight Center*
[b] *Mechanical and Aerospace Engineering Department, University of Alabama in Huntsville*

Abstract

This work explores the parameter space of a cylindrical hybrid nuclear fuel in support of a z-pinch driven pulsed fission-fusion (PuFF) engine. 0D power balance and 1D burn wave calculations have been performed to explore the parameter space of hybrid cylindrical nuclear fuels. The boundary of minimal initial conditions needed to reach breakeven are found within the context of the model. The effects of initial conditions upon the yield at the end of burn wave expansion are also determined. The model is used to examine the minimum initial energies predicted to result in yields of a few MJ. The goal of this work is to guide fuel design, inform future models and experiments as well as look for the most efficient parameter space for ignition in a z-pinch driven hybrid nuclear reaction. The impact of initial parameters upon ignition, burn, and gain are discussed. It is found that a hybrid cylindrical target may breakeven with initial energy near the axis of approximately 4 to 6 MJ in lithium deuteride/uranium 235 fuel. It is also found that magnetic field can lower the threshold further of which the magnitude changes across the parameter space. The dual fusion/fission reactions are found to boost each other leading to lower initial driving energies needed to reach breakeven in the hybrid cylindrical nuclear fuel.

Keywords: `Nuclear, Fission, Fusion, Advanced Propulsion`

1. Introduction

Nuclear fusion has great potential for access to massive quantities of energy from small amounts of fuel. Nuclear reactions have specific energy on the

order of 8×10^7 kJ kg^{-1}. In comparison chemical systems are limited to approximately 14 kJ kg^{-1}. It has; however, been notoriously difficult to achieve a working fusion power plant due to many hurdles in technology and physics such as magnetohydrodynamic instabilities, material limitations, and driving power technology. Still, access to nuclear fusion power would not only be a game changer in terms of terrestrial power generation, but also in space flight propulsion systems.[1]

Research into fusion energy has focused primarily on two regimes; Inertial Confinement Fusion (ICF) and Magnetic Confinement Fusion (MCF). ICF generates fusion reactions through pulsed implosions of pellets. The inertial forces drive the fuel to high density and temperatures. MCF seeks to generate fusion reactions by confining a low density plasma via magnetic field at steady state. There is a wide range separating the parameter space between ICF and MCF regimes. In fact the difference in density differs by approximately 10^{11}. Magneto Inertial Fusion (MIF) sometimes referred to as Magnetized Target Fusion (MTF) operates in the intermediate parameter space between these regimes and may lead to a scheme that can reduce the severe demands of breakeven fusion reactions.[2] MTF is a nascent field in comparison to ICF and MCF. However, there are some that have and are continuing to explore this portion of the parameter space.[2, 3, 4, 5] Early on in fusion research it was recognized that a magnetized fuel could be useful in improving yield. The presence of a magnetic field in the fusion plasma aids in retaining alpha particles in the burning region allowing more of their energy to be deposited into the plasma and increase temperature.[4] The magnetic field can also have a stabilizing effect leading to increased confinement times. A good overview of MIF is given by Kirkpatrick.[5] Lindemuth et al. have explored the thermonuclear fuel parameter space and examined MIF while comparing it to MCF and ICF. In this they also conclude the MTF may offer a route to accessing breakeven fusion at intermediate density regime with relatively lower power drivers.[2, 4] It should also be mentioned that in recent years Sandia has made progress in studying MIF for terrestrial power and has conducted several important experiments on the Z Machine.[6].

The energy to weight content of fusion fuels could lead to propulsion systems that are many orders of magnitude more efficient than current chemical engines. Unlike current electric propulsion systems, nuclear fusion propulsion would maintain a relatively high thrust value and specific energy.[1] Development of these propulsion systems suffer from the same limitations of terrestrial power fusion systems in addition to the limitations of space flight hardware such as mass and volume.

The goal of many scientists and engineers that are interested in advanced propulsion systems is to develop a system that can access a high specific energy process such as nuclear fusion while limiting the size and mass of the system such that it can be fielded for deep space exploration. Increasing the efficiency and specific power of deep space propulsion, often measured by specific impulse (s) and alpha ($\frac{kJ}{kg}$), would pave the way for large scale robotic and manned exploration throughout the solar system.

1.1. Recent Research in Nuclear Propulsion

Fission propulsion is often viewed as a more near term technology than fusion propulsion. The NERVA program completed tests of several experimental reactors for nuclear thermal propulsion. This program obtained a lot of useful data prior to cancellation due to politics and restrictions on nuclear testing. Interest in nuclear thermal propulsion has been revived recently. Work in this area is being performed by NASA Marshall Space flight Center in partnership with the Department of Energy.[7] This work includes system and programmatic studies, the development of ground testing capabilities[7], and fuel element materials research[8, 9].

Important research has also been pursued in recent years on a variety of fusion propulsion concepts. Plasma Jet Magneto Inertial Fusion (PJMIF) is an interesting concept that involves many jets of magnetized plasma converging to form a reacting fusion spheroid. Work in this area is on going and must not only develop the jets but also achieve the formation of the magnetized plasma spheroid.[10] A significant system study of a spherical torus concept has

also been proposed that is analogous to the film "2001: A Space Odyssey. This included a detailed estimate of many vehicle systems and predicted an alpha of 5 to 50 $\mathrm{kW\,kg^{-1}}$. This system must reject large amounts of heat due to the power conversion cycle which equates to significant mass penalties. The relatively low density of the magnetic confinement system also limits the minimum size of the reactor.[11] The Icarus project and its predecessor Daedalus set out to design a vehicle for interstellar trips to Barnard's star and Epsilon Eridani. These systems largely pursued inertial confinement fusion propulsion similar to fusion research conducted at the National Ignition Facility. This concept suffers from severe instabilities and inefficient drivers. This results in difficulty reaching ignition and drives the design to very large systems.[12] A direct drive fusion engine is actively being studied by Razin[13]. It employs a steady state field reversed configuration (FRC) plasma to heat propellant before expanding it through a magnetic nozzle. While this is certainly an interesting concept the lower operating density of steady state confinement systems limits size and power. The system is estimated to produce 40 N of thrust and have a specific power of $0.18\,\mathrm{kW\,kg^{-1}}$. Also, a thermonuclear microbomb concept has been proposed by Winterberg [14] in which a large portion of the spacecraft is a giant gigavolt capacitor. The capacitor discharge sparks ignition in a DT (Deuterium-Tritium) capped DD(Dueterium-Deuterium) cylindrical fuel via a proton beam. This would ignite a burn wave propagating the length of the cylinder which deposits energy into surrounding hydrogen. This plasma is then used to produce thrust. Developing the power system and overcoming limitations in capacitor technology as well as integrated system impacts upon the rest of the integrated vehicle are among the obstacles that this concept must overcome.

The authors and their affiliates at Marshall Space Flight Center and the University of Alabama in Huntsville have been working on a research effort to develop a pulsed fission-fusion (PuFF) propulsion system. This is a hybrid nuclear system that operates in the magneto inertial fusion regime and includes a combination of fission and fusion fuel.[15] Previous studies of the system estimate the potential specific impulse and alpha to be 20 000 s and $15\,\mathrm{kJ\,kg^{-1}}$

respectively. Thrust capability is estimated at 20 kN. [15]

Hybrid systems employ both fusion and fission processes to achieve a gain in energy. The nuclear processes, such as heat and neutron production, boost each other's reaction rates which increases energy production. Fission reactions provides additional heating to the fusion fuel. Increasing the temperature of the fusion fuel increases the reactivity and reaction rate. The fusion reactions in turn generate a flux of neutrons through the fission fuel leading to a boost in fission reactions. Together in a hybrid system this develops into a positive feedback loop boosting overall energy production. The boost in reactions due to the hybrid fuel should lower the requirements to reach positive energy production thereby not only making it easier to achieve adequate gain but also to reduce the size of the supporting subsystems. Hybrid nuclear propulsion has been studied previously by Winterberg.[16] Winterberg proposes a hybrid fuel dense plasma focus that uses fissionable material to ignite and boost DT reactions and initiate a burn wave Outside of the work by Winterberg and Cassibry, little mention of hybrid propulsion concepts exist in the literature.

There are many obstacles to developing a PuFF system. The work described below seeks to explore the parameter space as a precursor to more resource intensive modeling which will seek to characterize the fuel and implosion processes. Fuel characteristics such as geometry and materials are explored in the context of finding minimum energies for ignition. This work is intended to advance knowledge of the PuFF fuel and implosion as well as assist in the design of experiments.

1.2. Z-Pinch Stability

The z-pinch, employed by the PuFF system discussed above, is an inherently unstable process. Several mechanisms exist that distort and disrupt the idealized cylindrical pinch resulting in a turbulent mixing process that limits confinement and compression. One of the primary instabilities that must be mitigated is the Magneto Rayleigh Taylor Instability. This instability arises from a lower density fluid accelerating a higher density fluid. In the case of the z-pinch, the magnetic

field acts effectively as a zero density fluid accelerating a plasma of finite density. The instability begins with a sinusoidal perturbation in the surface which quickly devolves into severe distortion and mixing. Additional instability mechanisms exist. An example of an additional mechanism would be the Kelvin Helmholtz Instability that results from velocity shear in a fluid. These multiple mechanisms can combine and work together to limit the implosion and confinement of the z-pinch.

The instabilities fighting the pinch must be mitigated to the extent necessary to achieve the required density, temperature, and confinement requirements. Several mitigation strategies have been explored in recent years. Application of these strategies may be incorporated into z-pinch systems to improve stability.

It has been shown by Sandia and Los Alamos National Laboratories in Magnetized Liner Inertial Fusion (MAGLIF) experiments that axially premagnetized imploding liners form a helical structure and exhibit improved stability relative to non axially premagnetized imploding liners.[17] Additional work at Sandia National Laboratories has shown enhanced implosion stability in magnetically accelerated liners that are coated in a dielectric. The dielectric is understood to suppress electrothermal instabilities at the surface of the liner which seed the Magneto Rayleigh Taylor Instability, thus delaying the onset.[18] Researchers at the University of Washington have shown extended stability in experiments with their test facilities "ZaP" through sheared axial flow. The shear axial flow disrupts the formation of unstable perturbations of the z-pinch.[19] Additionally, improved stability has been seen in staged or structured z-pinches that use distinct layers of plasma in which outer layers implode upon inner layers. The relative nature of the plasma and the changing acceleration profile from multiple layers impinging upon each other can provide increased stability.[20, 21] Stabilizing mechanisms such as these should be considered for integration into z-pinch systems, such as PuFF, in order to improve stability and promote the formation of a stagnation state at the end of the implosion capable of igniting the thermonuclear reactions.

1.3. Modeling and Analysis of MIF Systems

Modeling and analysis is an important tool in gaining insight into the implosion of a MIF system. The process is highly coupled and complex. It includes magnetohydrodynamics, instabilities, and energy production and loss mechanisms. Much of historical modeling and analysis has been focused on ICF implosions.[22, 23] Atzeni et al. have studied ignition in ICF fuels and the propagation of burn waves.[24] Achieving ignition in a hot spot and initiating a burn wave is significant in that it is far less energy intensive than heating the entire fuel. In previous analysis, a burn wave propagating into a cold fuel is studied along with the various energy production, loss mechanisms and dynamics. Atzeni finds that ignition is favored by higher temperatures and larger ratios of cold to initial hot spot density. Atzeni also identifies ignition regions for given initial conditions and defines an ignition curve in the T,ρR space which divides the initial conditions leading to ignition from those that are quenched.[25, 24] More recently individuals at Sandia National Laboratory, including Slutz and Vesey, have studied MIF in the context of the magnetized liner inertial fusion (MagLIF) program. They show that high gain is possible in liner implosions acting on magnetized fuels with a inner layer of cold denser fuel into which a burn wave can propagate.[26]

1.4. Pulsed Fission-Fusion Research

Similar to the work of others previously described, the effort reported below seeks to explore the MIF parameter space in the context of a PuFF engine. The effort seeks to shed light on the characteristics of the fuel and implosion to guide the design toward more efficient ignition and burn. Little work has been done to explore MIF of hybrid nuclear systems. This is especially so for nuclear space propulsion systems. The authors and affiliates are interested in hybrid nuclear reactions because they potentially lower the aerial density (ρR) and temperature thus lowering the driver mass for the reactor. The idea for the hybrid approach[15] came from discussions regarding the number of launches needed to boost and assemble a fusion propulsion system in orbit, and is an

outgrowth of earlier pure fusion z-pinch work summarized in Polsgrove et al[27] and Meirnek et al[28]. The successful development of a PuFF engine would enable significantly large payloads and faster transit times throughout the solar system.[1, 15] The PuFF engine concept has roots in the NASA HOPE study conducted in 2003[29] and earlier pulsed z-pinch work.

The remainder of this document describes the approach in section 2, the results in section 3, discussion in section 4 and concluding remarks in section 5.

2. Approach to 1D Burn Wave Calculations

Calculations were performed in a simplified one dimensional model of a cylindrical hybrid nuclear fuel. They were set up to test the initial conditions near the axis leading to a burn wave propagating radially outward. The geometry and materials were chosen to represent an approximation to the nuclear fuel of the PuFF engine described above. The results of this model are intended to contribute to the design of the PuFF fuel and inform more robust modeling. The geometry is sketched in Figure 1. This figure illustrates a core of fusion fuel surrounded by a layer of fissile fuel and a propagating burn wave near the axis.

2.1. Governing Equations

2.1.1. Power Balance

A power balance is required in both a time dependent one dimensional burn wave model as well as in a zero dimensional time independent parameter space survey. Energy gained and lost must be accounted for in the power balance of the system.

$$\begin{aligned} P_{total} = P_{Fusiontotal} + P_{fission} - Q_{brehm} \\ -Q_{sync} - Q_{cond} - W_{mech} \end{aligned} \tag{1}$$

Mechanisms such as bremsstrahlung radiation, Q_{brehm}, synchrontron radiation, Q_{sync}, conduction, Q_{cond} and mechanical work, W_{mech} remove energy

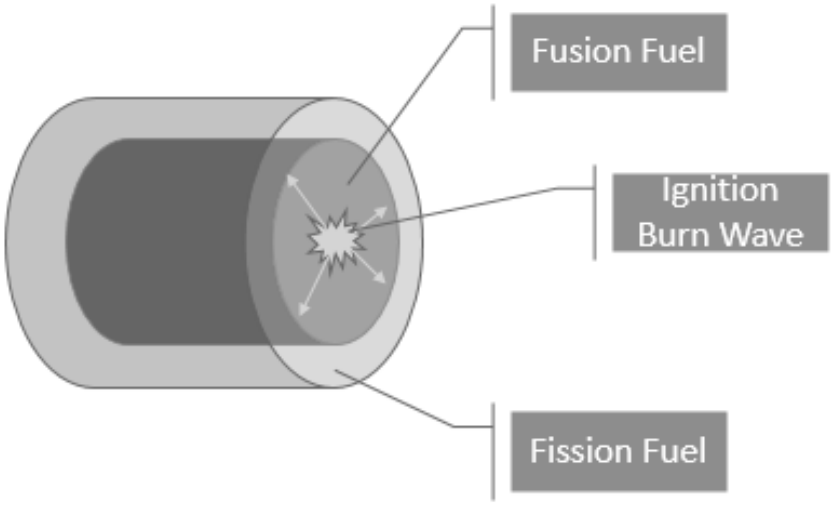

Figure 1: Diagram of Modeled Geometry and Burn Wave. The fuel capsule is approximated as a cylinder.

from the system. Fusion power, $P_{Fusiontotal}$, and fission power, $P_{fission}$, produce energy in the system. All of these processes contribute toward the total power, P_{total}, being produced in the system. The summation, when positive, indicates that more power is being produced than consumed and is therefore past the breakeven point.[24]

Fusion power can be broken down into the contributions from charged particles and neutrons.

$$P_{Fusiontotal} = \sum_{i=0}^{total} f_{\alpha i} P_{CPi} + \sum_{j=0}^{total} f_{nj} P_{Nj} \tag{2}$$

The power from nuclear reactions captured in the plasma is a summation of the power produced by charged particles,P_{CPi}, and neutrons,P_{Nj}. These terms are multiplied by the fraction deposited in the fuel,f, to determine the contribution to the energy gained in the system.

2.1.2. Energy Production

Fusion Energy. The fusion of two lighter nuclei into one heavier nuclei occurs at high energies and densities. The reaction rate can be determined by first calculating the reactivity, σv. Then multiplying the reactivity by the densities, n, of the two species and the volume, V.[24]

$$\frac{dN}{dt} = \frac{n_1 n_2}{1+\delta_{12}} V < \sigma v > \tag{3}$$

$$P_{CP} = \frac{dN}{dt} N_{cp} E_{cp} \tag{4}$$

The reaction rate, $\frac{dN}{dt}$, can then by multiplied by the number of charged particles per reaction , N_{cp}, and the energy of the charged particles, E_{cp}, to determine the total power, P_{cp}, produced. The charged particles were averaged for the multiple reaction outcomes. The fusion power produced by charged particles must then be multiplied by a factor representing the fraction deposited into the plasma by the charged particles since some of the energy is inevitably allowed to escape the system.[24]

There are many potential reactions that can occur in DLi^6 fuel. For this analysis, reactions with lower reactivities are neglected. Relevant reactions include:[30]

$$D_1^2 + T_1^3 \dashrightarrow He_2^4(3.5MeV) + n(14.1MeV) \tag{5a}$$

$$D_1^2 + D_1^2 \dashrightarrow T_1^3(1.01MeV) + p(3.02MeV) \tag{5b}$$

$$D_1^2 + D_1^2 \dashrightarrow He_2^3(0.82MeV) + n(2.45MeV) \tag{5c}$$

$$D_1^2 + Li_3^6 \dashrightarrow 2He_2^4(22.4MeV) \tag{5d}$$

$$D_1^2 + Li_3^6 \dashrightarrow He_2^3 + He_2^4 + n + 2.56MeV \tag{5e}$$

$$D_1^2 + Li_3^6 \dashrightarrow Li_3^7 + p + 5MeV \tag{5f}$$

$$D_1^2 + Li_3^6 \dashrightarrow Be_4^7 + n + 3.4MeV \tag{5g}$$

In a similar process the reaction rate should be multiplied by the number of neutrons per reaction, the neutron energy, and a neutron deposition factor. This

determines the amount of neutron energy deposited into the plasma. Together the energy deposited by the charged particles and neutrons accounts for the total contribution from fusion of energy addition to the system.[24]

$$P_N = \frac{dN}{dt} N_{neutron} E_{neutron} \tag{6}$$

Fusion reactivity is calculated based on R-matrix cross sections as described in the Naval Research Laboratory (NRL) Plasma Formulary.[31] In the case of DLi^6 fuel the reactivity is interpolated directly from a table of published empirical values.[32] The equations for reaction rates can be found in *The Physics of Inertial Fusion* by Atzeni.[24]

Secondary Reactions. Secondary reactions such as the production and burn of Tritium can contribute a significant amount of energy to the system. In the case of DLi^6 fuel the neutron flux from the fission reactions traveling back through the fusion fuel is used to calculate a tritium (H^3) production rate. This follows the same procedure as is described in 2.1.2. This process is a source of energy. The tritium reaction with deuterium can then be calculated using the process described in 2.1.2. So for a DLi^6 fusion fuel there are five energy production mechanisms; DLi^6, DD, Fission, Tritium Production, and DT reactions.

Fission Energy Production. In a hybrid nuclear target the fission processes generate heat and produce an additional neutron flux that drives the temperature of the fusion fuel higher, thus making it easier to reach temperatures for ignition with smaller drivers. Note that spontaneous fission, especially in the presence of an external neutron source could make a significantly greater contribution and further lower the driving requirements of the system. In this work, fission reactions are calculated as a function of the neutron flux from the fusion reactions and spontaneous fission is neglected.[33] Some fraction of the neutron flux causes fission which then produces energy and more neutrons. The addition of energy in this way heats the fusion fuel thus increasing reaction rates. This should be a conservative estimate for fission reactions. Taking into account spontaneous

fission especially if there is an external neutron source would increase fission reactions and the reactivity of the fusion fuel, thus lower the requirements of delivered energy and density that need to be reached to breakeven.

The fission reaction rate is in part determined by the cross section. This property of the element represents the likelihood of a fission event occurring during an encounter with a neutron. The first step in calculating the fission reaction rate from the neutron flux is to find the macroscopic cross section (represent by capital σ_{fast}) as a function of cross section (σ), fuel density, $n_{fission}$, and a unit conversion from barns to cm^2.[33]

$$\Sigma = \sigma_{fast} n_{fission} 10^{-24} (\frac{cm^2}{barn}) \tag{7}$$

The volume of the layer of fission fuel can be found from simple geometry of a cylinder where r is the radius.

$$V_{fission} = \pi (r^2_{fissionfuel} - r^2_{fusionfuel}) l \tag{8}$$

The neutron flux passing through the fission fuel can be found from the fusion reaction rate. This needs to be multiplied by the time step of the calculation, dt, to determine the number of neutrons produced during that time step. Then this must be multiplied by the number of neutrons produced per reaction, ν, the velocity of the neutrons, v_ν, and the inverse of the fission fuel volume. This must be done for each of the fusion reaction rates in cases where multiple fusion reactions are occurring simultaneously as with DLi^6. Due to the velocity term, this actually results in a flux rate term in units of neutrons per unit area per unit time.[33]

$$N_{fluxrate} = \frac{dN}{dt} dt (\frac{\nu v_\nu}{V_{fission}}) \tag{9}$$

A portion of the neutron flux is lost out the ends of the cylinder, thus this can be taken into account with an end loss term that is a ratio of the outer area of the fission fuel cylinder to the area of the end surfaces. The end loss ratio is

multiplied by the neutron flux to determine the portion of the flux transmitted toward the fission fuel.

$$Endloss = \frac{2\pi rl}{2\pi r^2 + 2\pi rl} \tag{10}$$

One can now calculate the rate of fission reactions. The macroscopic cross section when multiplied by the flux and volume of the fission layer gives the time rate of fission reactions. This can be scaled by an enrichment term,ϵ.[33]

$$\frac{dF}{dt} = \Sigma \epsilon N_{fluxrate} Endloss V_{fission} \tag{11}$$

Finally the fission power produced is found by multiplying the rate of fission reactions by the energy per fission reaction.[33]

$$P_{fission} = \frac{dF}{dt} E_{perfission} \tag{12}$$

Energy Transfer from Fission Fuel. A significant amount of energy is generated in the fission fuel. Some of this will transfer to the fusion fuel through neutron products and will contribute to heating it. For the purposes of this analysis each fission event is assumed to produce 3 neutrons carrying 5 MeV of the fission energy.[33] The partial deposition of fission neutron energy into both the cold and hot fuel is accounted for in the calculations. This results in significant heating of the fusion fuel which boosts reactivity.

Cold Fuel Heating. The cold fuel, in addition to being heated by the fission reactions, is also heated by the alpha particles escaping the hot spot. A fractional deposition term is calculated for the cold fuel and multiplied by the alpha particle energy escaping the hot spot.

$$P_{coldfuelheating} = \sum_{i=0}^{total} (1 - f_{\alpha i}) f_{coldfueli} P_{CPi} \tag{13}$$

Fractional Energy Deposition Terms. The energy of the reaction by products must be scaled by deposition terms as referenced above. Only a portion of the energy produced is captured within the plasma through collisions, and the rest is lost to escaping particles. Fractional deposition terms are found to determine the amount of energy deposited into the system for both neutrons and alpha particles.[24]

The fraction of energy deposited by neutrons is related to the multiple of density and neutron mean free path. This is a similar order of magnitude for dense plasmas and can be approximated as areal density, ρR. The fractional neutron term can be approximated as shown.[24, 34]

$$f_n = \frac{\rho R}{\rho R + 200} \tag{14}$$

The fractional deposition of alpha particles is found by simplifying the model to the primary energy loss process. In the energy range of a few 10's of keV the largest contribution to α particle stopping comes from small angle collisions with electrons.[35] It is assumed that the characteristic time for energy deposition and the electron-ion equilibration time are equal since their magnitudes are approximately equal. Electrons and ions are therefore assumed to have the same temperature. It is assumed here that alpha particle energy is deposited instantaneously. The fraction of α particle energy deposited is then defined as.[36]

if $\tau <= 0.5$

$$f_\alpha = \frac{3}{2}\tau - \frac{4}{5}\tau^2 \tag{15}$$

if $\tau > 0.5$

$$f_\alpha = 1 - \frac{1}{4\tau} + \frac{1}{160\tau^3} \tag{16}$$

The fractional deposition of the α particle is found with the τ function, which is a ratio of the radius (r_{hot}) of the hot reacting portion of the fuel and the distance traveled by the α particle.[36]

$$\tau = \frac{r_{hot}}{\lambda}(1 + \frac{r_{hot}}{r_{larmor}}) \tag{17}$$

The τ equation is a function of temperature, T, number density, n, alpha particle mass, m_{alpha}, alpha particle velocity, $v_{velocity}$, magnetic field, B, alpha particle charge, Z, and the charge of an electron, q_e as derived from the Coulomb logarithm, the mean free path, and the larmor radius.[24]

$$\lambda = \frac{1.07T_{keV}^{\frac{3}{2}}}{\Lambda m_a n} \tag{18}$$

$$\Lambda = \ln(\frac{1.24e^7 T^{1.5}}{\sqrt{n}Z^2}) \tag{19}$$

$$r_{larmor} = \frac{m_{alpha}v_{alpha}}{Z_{alpha}q_e B} \tag{20}$$

2.1.3. Energy Lost

Thermal Conduction. Thermal conduction is one of the dominating mechanisms of energy loss in fusion systems. In this work, the change in radius over which the thermal conduction is assumed to take place is $dr = \frac{r}{10}$. The thermal conduction is seen in equation 21.

$$Q_{cond} = \kappa \frac{T_{hot}}{dr}(2\pi r_{hot} l + 2\pi r_{hot}^2) \tag{21}$$

Where T is temperature of the hot spot, r is radius of the hot spot, and κ is the thermal conductivity.[37] Thermal conductivity is found using Braginskii's coefficients. This relationship can be seen in equations 22 and 23.

$$k_{electron} = \frac{nk_b^2 T\tau}{m} \frac{4.66(\omega\tau)^2 + 11.92}{(\omega\tau)^4 + 14.79(\omega\tau)^2 + 3.77} \tag{22}$$

$$k_{ion} = \frac{nk_b^2 T\tau}{m} \frac{2(\omega\tau)^2 + 2.64}{(\omega\tau)^4 + 2.7(\omega\tau)^2 + 0.68} \tag{23}$$

Where $k_{electron}$ and k_{ion} are the thermal conductivities for electrons and ions respectively, k_b is the boltzmann constant, T is the temperature, τ is the collision time for the relevant particle, ω is the cyclotron frequency and n is the number density of the particle.

Particle	Electrons	Ions
Temperature (keV)	5	5
Density (n/m^3)	$1.5055e^{29}$	$1.5055e^{29}$
Avg. Charge Number	1	2
Avg. Atomic Number	N/A	4
Magnetic Field (T)	0	0

Table 1: Plasma conditions defined for a calculation of the physical scale of heat transfer in the hot fusion plasma.

Conductivity	W/Kcm^2
Electron Thermal Conductivity	46.92
Ion Thermal Conductivity	0.0493
Total Thermal Conductivity	46.9693

Table 2: Calculated Thermal Conductivities

Analysis of the Thermal Scale. An analysis of the physical scale at which thermal energy is transported through the fusion fuel can be performed through calculations of thermal conductivity and thermal diffusivity. Equations 22 and 23 can be used to calculate the specified plasma conditions. A sample calculation was run at conditions listed in table 1. Where the computed values of thermal conductivity are given in table 2. Thermal diffusivity can then be calculated with equations 24 and 25.

$$\alpha = \frac{k}{\rho C_p} \tag{24}$$

$$C_p = \frac{\gamma R}{\gamma - 1} \tag{25}$$

Where ρ is the mass density, C_p is the specific heat at constant volume, γ is the ratio of specific heats, and R is the specific gas constant. Now if we define a relevant time scale to be 1 ns, then we can compute the physical scale over which heat is transferred on that time scale with equation 26. When the

physical scale is calculated with these values a scale of approximately 80 µm is found.This scale length is significantly smaller than the size of the initial hot spot in the calculations. Thus over the relevant time scales thermal energy does not significantly diffuse out of the hot spot region.

$$dr = \sqrt{t\alpha} \tag{26}$$

Radiation Losses. Radiation losses play an important role in the energy balance of a hot plasma. In this model, two radiation mechanisms are calculated; Synchrotron[38] and Bremsstrahlung[24]. The radiation equations are functions of density, temperature, magnetic field and geometry.

$$Q_{sync} = 5.342866e^{-24}B^2 n_e T_{hot}(1 + \frac{T_{hot}}{2.36727e^9}) \tag{27}$$

$$Q_{brehm} = 1.445e^{-40} n_e T_{hot}^{\frac{1}{2}} n_i V \tag{28}$$

Mechanical Work. Mechanical work is an additional loss mechanism that comes from the expansion of the hot spot due to pressure and a change in volume.[24]

$$dV = \pi(r_1 - r_0)l \tag{29}$$

$$W_{mech} = \frac{PdV}{dt} = \frac{\rho_{hot} R T_{hot} dV}{dt} \tag{30}$$

2.1.4. Burn Wave Propagation

The function from which the burn wave velocity is calculated is derived directly from the perfect gas equation of state, continuity and momentum equations in the case of a moving shock wave. It is dependent upon the temperature, density, and molecular characteristics of the gas before and after the shock wave.[39]

$$v = \sqrt{\frac{(\rho_{hot} R T_{hot} - \rho_{cold} R T_{cold})}{\rho_{hot} - \rho_{cold}} \frac{\rho_{cold}}{\rho_{hot}}} \tag{31}$$

Note that as the temperature of the cold fuel approaches that of the hot fuel the velocity of the burn wave drops toward zero. When velocity is sufficiently low the entire fusion fuel is assumed to be in the hot spot.

2.2. Initial Conditions and Assumptions

This work examines one of two families of pulsed fission fusion engine target types. The PuFF engine uses a hybrid reaction consisting of both fission and fusion reactions. This hybrid nuclear process will lead to a primary and secondary reaction in terms of energy production. The first family of targets produces the majority of energy from fission reactions and the fusion reactions serve to boost the fission process. The energy production in the second family of targets is dominated by fusion reactions and boosted by the fission products. This study focuses on the second family of targets.

The calculations assume a geometry with defined radii for fusion and fission fuel and a length equal to the radius of the fusion fuel. The initial hot section is a cylinder centered on the axis with a radius equal to 10 % of the fusion fuel radius. An initial energy is defined for the hot spot and the temperature is calculated assuming a perfect gas with constant specific heat. While the initial hot spot cylinder radius will change the temperature, it will also change the reacting mass. The change in temperature and reacting mass should result in the model being somewhat insensitive to the initial hot spot cylinder radius.

In addition to the geometry and hot spot energy, a constant magnetic field is defined. The cold fuel regions are assumed to be room temperature, which is effectively negligible, at $t = 0$ s. The material properties (e.g. cross section, particle mass, molecular weight) are defined as well. For the purposes of this work the materials were limited to lithium deuteride for the fusion fuel and uranium 235 for the fissile fuel.

The fission fuel density was assumed to be solid density, removing the need to estimate the compression of uranium. Three density profiles were chosen for the fusion fuel that are each an exponential function of radius. In each case the max compression is at the axis and the density drops to about solid density at

the edge of the lithium deuteride. This exponential radially decreasing density profile is similar to post shock reflection off the axis. Maximum density ratios at the axis are 5, 10, and 20, Fig. 2.

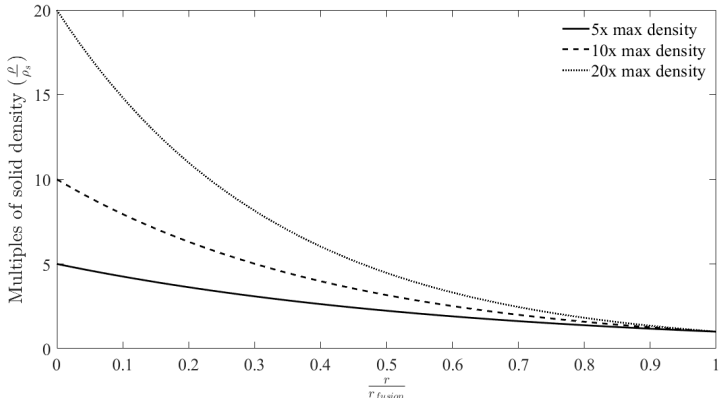

Figure 2: Density Profiles Examined in Analysis

2.3. Analysis Products

The analysis described generates 0D contour plots in $T - \rho R$ space in which contour lines represent the boundary at which breakeven is achieved. Graphs are also generated in which the conditions of the expanding hot spot are plotted in $T - \rho R$, $T - time$ and $Power - time$ space. Additionally the energy gained from $t = 0$ till the burnwave reaches near zero velocity or the edge of the lithium deuteride is calculated for the hot spot only and for the entire reacting mass, which included energy of the uranium.

2.4. Scope

The analysis focused on relatively small fuel cylinders as this will be more logistically feasible in the context of the greater PuFF system. Table 3 displays the geometries examined. The dimensions were estimated based on notional ideas of the fuel size. Radii of the fusion and fission fuels were varied to investigate the impact on breakeven requirements. Additionally, 0 Tesla and 100

Geometry Variations in Model (cm)			
Geometry	R_{Fusion}	$R_{Fission}$	Length
1	0.4	0.5	0.4
2	0.3	0.5	0.3
3	0.25	0.35	0.25
4	0.25	0.5	0.25
5	0.25	0.75	0.25
6	0.15	0.25	0.15
7	0.15	0.5	0.15
8	0.15	0.75	0.15
9	0.15	1	0.15

Table 3: Variations in Target Geometries

Tesla magnetic fields were considered. These conditions were chosen to explore the initial conditions leading to breakeven and small gains.

3. Results

3.1. 0D Power Balance

Prior to examining the results of the burn wave calculations it is worthwhile to look at the 0-D power balance of the system. This illustrates the dramatic difference fission makes in the hybrid reaction. In the 0-D power balance the same fundamental equations described above are applied to the first geometry, detailed below, in which the entire fusion fuel is at defined temperature and density conditions. From this a Lindl-Widner or temperature-areal density space contour plot is constructed. A grid of temperature and areal density points are input into the 0D power balance model to create the contour plot. The contours represent the boundary at which the reacting volume produces more energy than is lost.

One can see the power balance of a hybrid fuel plotted along side the power balance for both DT and DD pure fusion reactions in Figure 3. The magnetic

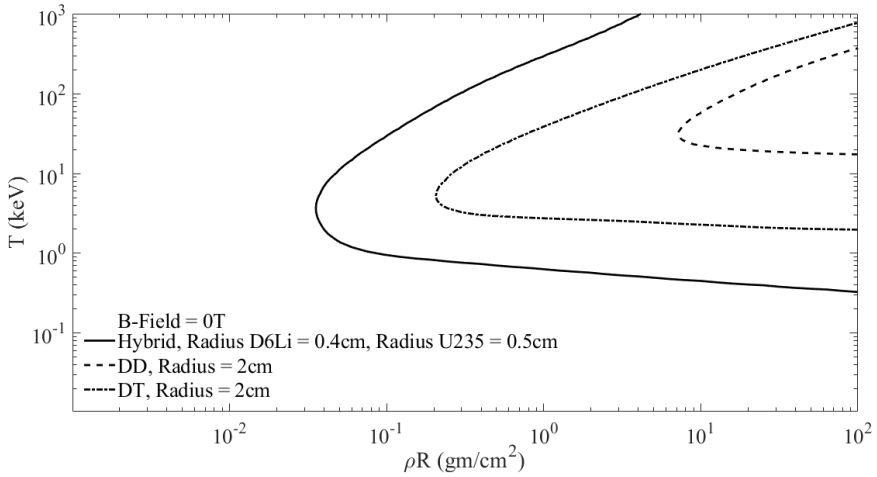

Figure 3: Power balance comparison between pure fusion and hybrid (fusion/fission) fuels

field is kept at zero in this plot. The breakeven line extends to the lowest energies and densities for a hybrid reaction in comparison with DD and DT reactions. Note that the fusion only reactions are calculated for a larger radius of 2 cm rather than the dimensions of geometry 1 due to the limitations of fusion only reactions in overcoming energy loss mechanisms.

For a given geometry the volume of fissile fuel is defined. The uranium liner is assumed to stay at solid density and therefore experiences no compression in order to keep the model more conservative and reduce variables. Neutron flux from DD and DLi^6 reactions passes through the uranium liner. A portion of the flux induces fission and thus neutrons, some of which pass back through the fusion fuel at the center and induce tritium breeding and DT reactions. The neutron flux is assumed to travel much faster than the time step of the model. The time step of the model is on the order of 1 nanosecond. The energy of the neutrons produced is approximately 2 MeV which relates to a velocity of approximately 2 $\mathrm{cm\,ns^{-1}}$. Thus the neutrons can traverse the system much faster than the time step of the model.

The fission reaction rate is dependent upon the cross section, which itself is a function of neutron energy. The neutrons in this environment will be fast or

highly energetic. The cross section for U_{235} is assumed to be a constant 2 barns for these calculations. Similarly the breeding of tritium is also based upon a cross section calculation. The cross section is a property of the material that determines the likelihood of interaction with the neutron. Higher cross sections result in more reactions. In the case of U_{235} the cross section is much lower for fast neutrons than for thermal. In the environment described most neutrons will not undergo enough scattering interactions to reduce their energy. As energetic particles collide with other particles, one may think of billiard balls on a pool table, they give up some of their kinetic energy to the impacted particle. This is often referred to as scattering. If scattering of the neutrons is significant, the average energy of the neutron in the system lowers considerably resulting in what are known as thermal neutrons. Thermal neutrons have a much higher fission cross section and would thus lead to far greater fission energy production. One can judge the significance of scattering by calculating the mean free path, the average distance a neutron would have to travel through the material before colliding or interacting with an atom. The mean free path of a neutron traveling through uranium is dependent upon density, energy as well as cross section and is many times greater than the scale length of this geometry even for modestly energetic neutrons. This indicates most neutrons are lost from the system before they interact with the uranium atoms in the liner.[33]

The work of Atzeni[24] shows similar boundaries for positive system energy production in the calculation of central ignition of pre-assembled fuel plotted in Lindl-Widner diagrams. Similarly, 1D calculations show the progression of hot spot temperature and areal density. The effect of cold fuel heating by an initially cooling hot spot is seen here as well. The hot spot then consumes the heated fuel and progresses into the region of net energy production. This work also shows hot spot initial conditions too far outside of the line of breakeven that result in cooling and failed ignition.[24]

As described above a magnetic field can have a noticeable effect in reducing the threshold breakeven conditions due to suppression of electron thermal conduction and trapping of alpha particles thus increasing alpha particle energy

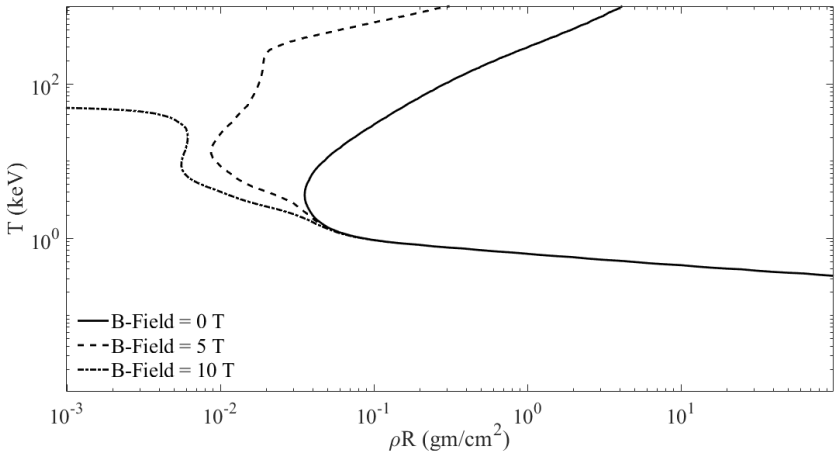

Figure 4: Power balance of a hybrid fuel with varying degrees of magnetic field

deposition. In the case of magnetized targets a noticeable effect is seen in Figure 4. The most dramatic effect is seen in the high temperature low areal density region of Figure 4. A few Tesla can be seen to extend the breakeven boundary above 1 keV to significantly lower densities. Below 1 keV the boundary drops a negligible amount in the high density low temperature region. Kirkpatrick's overview of magnetized target fusion[5] shows similar results in which a magnetic field greatly extends the region of net energy production into regions of lower density in agreement with Figure 4.[5]

In order to reach ignition, $\frac{dT}{dt} > 0$, the plasma cooling through radiation and conduction must be offset by the deposition in alpha particle energy. A study conducted by Basko, et al.[40] derives this and defines a ignition criteria of $BR \gtrapprox 6 \times 10^5$ G $-$ cm for low areal density magnetized DT fuels. The offset of plasma cooling is achieved when the alpha particles become magnetized such that the alpha larmor radius (equation 20) becomes comparable to the radius of the fuel, $r_{larmor} \approxeq r_{fusion}$.[40]

3.2. Ignition and Burn

The ignition and burn was assessed by applying the density profiles to the stated geometries while varying the initial energy in the hot spot region. Temperature, areal density, and energy production are examined for the expanding burn wave.

There are three different types of results. First, the initial energy is too low and while there is a propagating burn wave it does not produce as much energy as was initially in the system. Second, the initial energy is high enough to initiate a burn wave that rapidly consumes the cold fuel and rapidly grows the size and temperature of the hot spot region. Note that in the second case there is an initial drop in the energy of the hot spot that occurs prior to the consumption of adequate amounts of cold fuel. The hot spot at first cools before consuming enough fuel to overcome losses and rapidly increase in temperature. The third result takes place when the burn wave cools as it expands and consumes fuel but produces a relatively small amount (on the order of 1 MJ) of excess energy. This third scenario is more ideal for a PuFF type system that will have trouble redirecting a more energetic energy release with a magnetic nozzle.

In each case it is found that the given density profile has a minimum energy required to reach breakeven. Figures 5 and 6 present an example of the three result scenarios described above for Geometry 1.

In order to better understand the coupled nature of the hybrid reaction, the ratio of fusion to fission energy production was calculated and plotted over time in Figure 7. The figure clearly shows that the fusion energy dominates the reaction. The dominance of the fusion energy illustrates that the most significant role of the fission liner is to boost fusion reactions in the hot spot. A large spike in energy occurs at the end of the simulation. As the burn wave progresses in the simulation the surrounding cold fusion fuel is heated. There reaches a point at which the cold fuel is approximately the same temperature as the expanding hot region. At this point the entire fusion fuel is considered to be reacting and the simulation is terminated. Beyond this point in the simulation the continuation of the reaction will be contingent upon the continued confinement

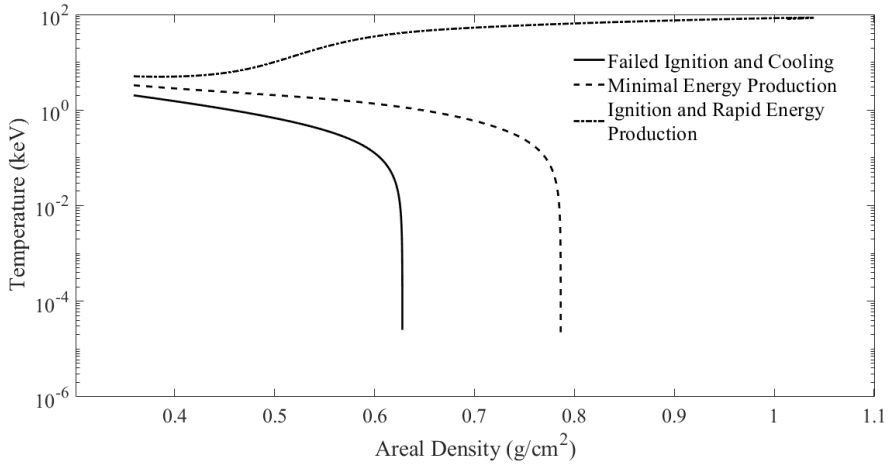

Figure 5: Lindl-Widner Plot of Geometry 1 undergoing ignition, marginal breakeven, and cooling reactions

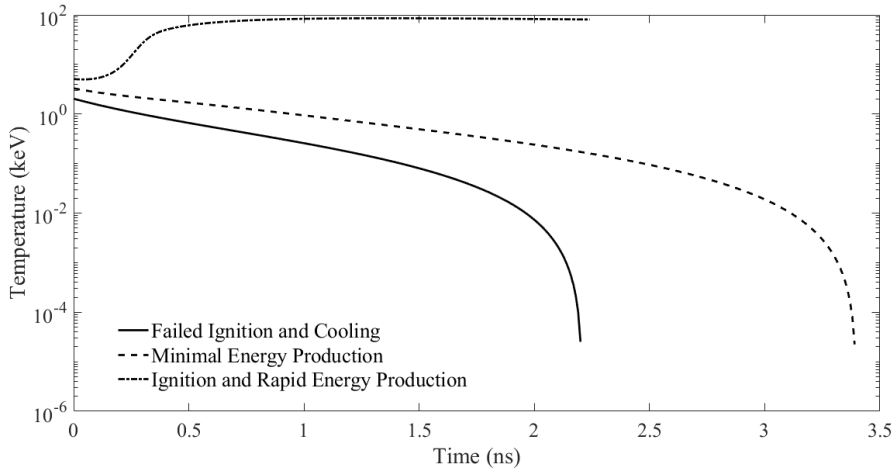

Figure 6: Temperature progression in time of Geometry 1 undergoing ignition, marginal breakeven, and cooling reactions.

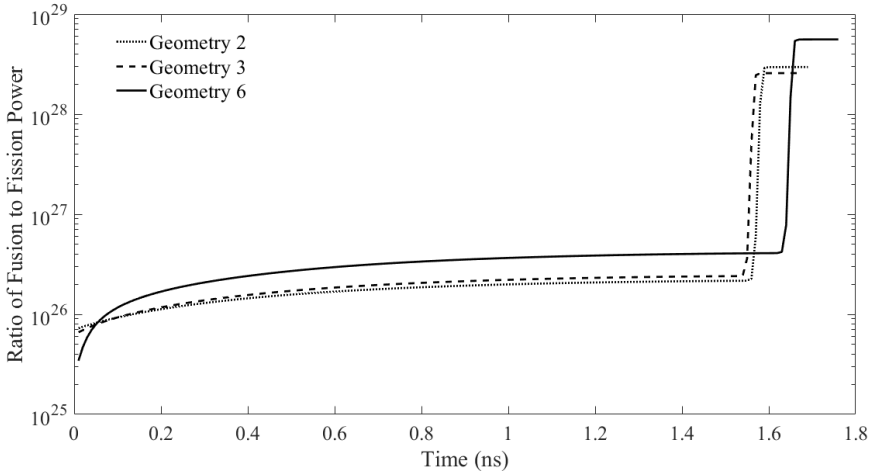

Figure 7: Ratio of fusion to fission energy production in 3 geometries at marginal breakeven conditions.

of the plasma. The confinement will be limited by the instabilities discussed earlier in this article and other transient processes that are beyond the scope of this model. Complete consumption of the fusion fuel by the hot spot is therefore considered to be the most well defined point at which to end the simulation for the purposes of this analysis.

3.3. Yield

One can examine the yield curve for different geometries near the breakeven point to assess the rate of change of yield beyond breakeven, the influence of magnetic field, and the impact of varying geometries. Figure 8 shows yield curve calculations for geometry 2 just above breakeven. One can see that the yield curve is steep beyond breakeven and therefore only small quantities of energy beyond the breakeven line result in large yield. Also, the addition of a 100 T magnetic field can be seen to increase the slope of the yield curve but does not greatly impact the point at which the system will breakeven. This corresponds to Figures 3 and 4 and is a result of the areal density regime in which the model reactions take place.

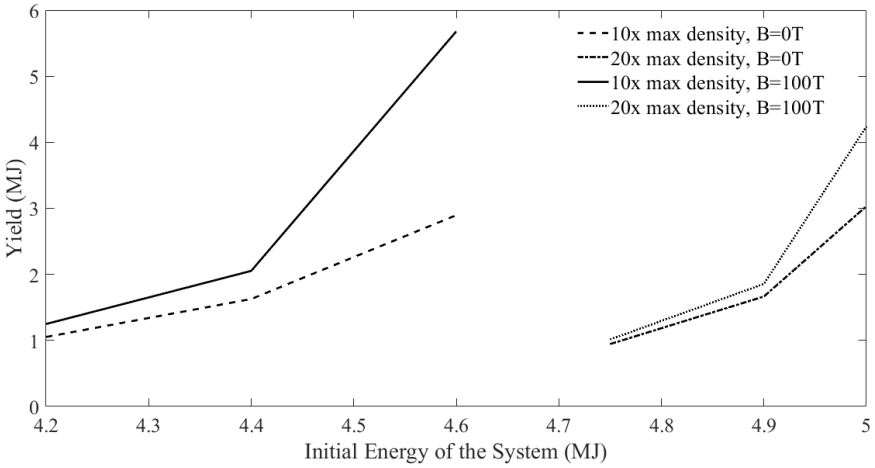

Figure 8: Yield for geometry 2 at two different compression profiles and two values of magnetic field.

4. Discussion

As seen above in section 3, geometry and magnetic field have an significant impact upon driving energy required for a hybrid cylindrical fuel to reach breakeven. The results presented above compare multiple geometries and density profiles along with magnetic field of 0 and 100 T.

As expected there is a minimum energy requirement that must be reached to initiate a burn wave that will produce more energy than was initially in the system. One should note a burn wave can still propagate without reaching breakeven. One can see (from 0 dimensional power balance, 1 dimensional burn wave models, as well as in the literature[24, 16]) the addition of fission reactions, seen below in 32a, considerably reduces the energy required to drive the fuel to breakeven when compared with pure fusion fuel. The drop in energy requirement is orders of magnitude lower. Note that the fission products P_1 and

P_2 are generic designations and vary statistically in the isotope produced.[33]

$$U + n \dashrightarrow P_1 + P_2 + \sim 3n \tag{32a}$$

$$Li_3^6 + n \dashrightarrow T_1^3 + He_2^4 \tag{32b}$$

The fission reactions heat the fusion fuel and, in the case of lithium deuteride, breed tritium from the lithium 6 (see reaction listed above in 32b) thus increasing the reaction rate. This in turn increases the neutron flux through the fissile material which increases the fission reaction rate. The two processes boost each other and produce far greater energy than they would alone. One can see that the fusion energy dominates the power production. The primary role of fission is to increase the quantity of fusion reactions rather than provide additional heat. One should note that this is only one variant on the fission/fusion hybrid. Other reactions dominated by fission processes may yield different results and trends.[30]

In studying the yield curve of multiple geometries one can see a trend in the minimum initial energies required to breakeven relative to the geometries. The yield curve trends toward lower starting energies (as low as 1 to 2 MJ) as the fusion and fission fuel radii decrease. This trend occurs until a limit is reached in minimum reaction mass. Higher compression ratios near the axis result in the optimum target size decreasing.

The introduction of a 100 T magnetic field boosted yield when applied to the same conditions modeled in the 0 T cases although the energy at which the system breaks even was not greatly changed. The magnetic field does increase the slope of the yield curve thus significantly increasing yield for conditions beyond breakeven. The impact of the magnetic field is greater for lower density fusion fuels than what is modeled in this analysis. This agrees with the 0D results presented above in section 3.1.

This analysis suggests breakeven may be achieved in hybrid cylindrical fuel with driving energy of only 1-4 MJ. The burn wave and yield curve analysis suggest that increasing compression (with maximum mass and energy density

at the axis) and decreasing the cold fuel mass (while maintaining some minimal quantity of reacting mass) will result in the lowest initial system energy the must be delivered through an implosion and heating mechanism such as a z-pinch. The analysis also shows that hybrid targets such as those considered in the document potentially have an order of magnitude or more lower energy requirements than pure fusion systems.

5. Conclusions

The authors set out to develop a 0D power balance and 1D burn wave model of cylindrical hybrid nuclear fuel in order to gain insight into the initial system energy requirements to reach breakeven for multiple configurations. 0D power balance Lindl-Widner plots show that the hybrid fuels decrease the temperature and density required for breakeven by more than an order of magnitude. Also, it is shown that a magnetic field can further reduce these initial energy requirements but has the most impact for hot lower density fuels. The 1D burn wave calculations indicated that a driving energy of 4-6 MJ may be adequate to reach breakeven in a hybrid cylindrical fuel and achieve modest gains of 1-2 MJ. The analysis also indicates that minimizing cold fuel mass and maximizing mass and energy density on axis result in the minimal initial energy requirements. This insight informs future modeling efforts of the parameter space in which to explore. It also informs the endeavor to develop a pulsed power experimental facility of the approximate energy requirements that must be obtained.

Dynamic effects and phenomena such as the Rayleigh-Taylor Instability will play an important role in the implosion and burn of these hybrid fuels. These along with two and three dimensional effects are planned to be studied as a part of the PuFF program in more robust modeling efforts. Work is already underway at MSFC and UAH to employ a 2D, nonlinear, explicit, finite element software, originally developed by Lawrence Livermore National Laboratory, and a multiphysics smooth particle hydrodynamic code[41] to model the implosion, burn and expansion of a hybrid nuclear fuel plasma. This work is required to

inform the design of pulsed power experiments. In time, experiments will be carried out to anchor models, obtain hybrid target implosion and burn data, and seek to demonstrate a breakeven reaction through pulsed power z-pinches.

Acknowledgments

The authors would like to thank the leadership at Marshall Space Flight Center and the University of Alabama in Huntsville for their ongoing support and interest in this work. The authors would also like to thank the NASA Innovative Advanced Concepts (NIAC) program for their support. Last but not least, the authors are always appreciative of the continued support and understanding from family and friends.

References

[1] Cassibry, et al, Case and development path for fusion propulsion 52 (2) 595–612.

[2] I. Lindemuth, R. Siemon, The fundamental parameter space of controlled thermonuclear fusion`doi:10.1119/1.3096646`.

[3] Wurden, et al, Maneto-inertial fusion 35 69–77. `doi:10.1007/s10894-015-0038-x`.

[4] Lindemuth, Kirkpatrick, Parameter space for magnetized fuel targets in inertial confinement fusion 23 (3).

[5] P. 1st International Symposium for Evaluation of Current Trends in Fusion Research (Ed.), Manetized Target Fusion - An Overview of the Concept, Los Alamos National Laboratory.

[6] Gomez, et al, Experimental demonstration of fusion-relevant conditions in magnetized liner inertial fusion`doi:10.1103/PhysRevLett.113.155003`.

[7] C. P. G. Doughty, Review of nuclear thermal propulsion ground test options.

[8] B. V. Eades, Survey of fuel system options for low enriched uranium (leu) nuclear thermal propulsion.

[9] T. B. D. B. Taylor, Emrich, Investigation of a tricarbide grooved ring fuel element for a nuclear thermal rocket.

[10] S. et al., Project icarus: Analysis of plasma jet driven magneto-inertial fusion as potential primary propulsion driver for the icarus probe.

[11] W. et al., Realizing "2001: A space odyssey": Piloted spherical torus nuclear fusion propulsion 39 (6).

[12] L. et al., Project icarus: Optimization of nuclear fusion propulsion for interstellar missions.

[13] R. et al., A direct fusion drive for rocket propulsion.

[14] Winterberg, To mars in weeks by thermonuclear microbomb propulsion 30.

[15] e. a. Adams, Cassibry (Ed.), Developing the Pulsed Fission-Fusion (PuFF) Engine, Poc. Propulsion and Energy Forum.

[16] Winterberg, Fusion-fission-fusion fast ignition plasma focus.

[17] e. a. T.J. Awe, R.D. McBride, Observations of modified three-dimensional instability structure for imploding z-pinch liners that are premagnetized with an axial field.

[18] e. a. Awe, Experimental demonstration of the stabalizing effect of dielectric coatings on magnetically accelerated imploding metallic liners.

[19] e. a. Shumlak, Equilibrium, flow shear and stability measurements in the z-pinch.

[20] e. a. H. Sze, Magnetic rayleigh-taylor instability mitigation and efficient radiation production in gas puff z-pinch implosions.

[21] AIP (Ed.), Fusion in a staged Z-pinch.

[22] P. V. Martinez-Val, Eliezer, Fusion burning waves in proton-boron-11 216 142–152.

[23] H. K. Honda, Nakao, Burn characteristics of inertially confined d-3he fuel.

[24] Atzeni, Meyer-Ter-Vehn, The Physics of Inertial Fusion.

[25] Atzeni, Caruso, Inertial confinement fusion: Ignition of isobarically compresed d-t targets 80 B (1).

[26] Slutz, Vesey, High-gain magnetized inertial fusion`doi:10.1103/PhysRevLett.108.025003`.

[27] P. et al., Design of z-pinch and dense plasma focus powered vehicles.

[28] M. et al, Z-pinch fusion-based nuclear propulsion.

[29] Adams, et al, Conceptual design of in-space vehicles for human exploration of the outer planets.

[30] Pass, Fusion, and advanced fuel, reaction bibliography.

[31] N. R. Laboratory, Nrl plasma formulary.

[32] Howerton, An Integrated System of Production of Neutronics and Photonics Calculational Constants.

[33] Emrich, Principles of Nuclear Rocket Propulsion, Elsevier.

[34] Avrorin, Criterion for the explosion of an inertial thermonuclear target.

[35] F. et al., Thermonuclear burn characteristics of compressed deuterium-tritium microspheres.

[36] Krokhin, Rozanov, Escape of α particles from a laser-pulse-initiated thermonuclear reaction.

[37] S. H. L. S. S. L. Riley, Two-dimensional direct simulation of deuterium-fiber-initiated z pinches with detailed comparison to experiment.

[38] Hayakawa, Cyclotron radiation from a magnetized plasma.

[39] Anderson, Modern Compressible Flow with Historical Perspective, 3rd Edition.

[40] M.-T.-V. Basko, Kemp, Ignition conditions for magnetized target fusion in cylindrical geometry.

[41] C. Schillo, Smooth particle hydrodynamics modeling of magnetized target yield in plasma driven magneto-inertial fusion.